Supplemental material to this article can be found at:
http://dmd.aspetjournals.org/content/suppl/2024/11/01/dmd.124.001798.DC1
1521-009X/52/12/1388–1395$35.00
DRUG METABOLISM AND DISPOSITION
dx.doi.org/10.1124/dmd.124.001798
Drug Metab Dispos 52:1388–1395, December 2024

Candesartan Has No Clinically Meaningful Effect on the Plasma Concentrations of Cytochrome P450 2C8 Substrate Repaglinide in Humans[S]

Mikael O.W. Piha, Kristiina Cajanus, Marica T. Engström, Mikko Neuvonen, Troels K. Bergmann, Mikko Niemi, Janne T. Backman, Anne M. Filppula, and Aleksi Tornio

Integrative Physiology and Pharmacology, Institute of Biomedicine, University of Turku, Turku, Finland (M.O.W.P., K.C., A.T.); Bioanalytical Laboratory, Institute of Biomedicine, University of Turku, Turku, Finland (M.T.E.); Unit of Clinical Pharmacology, Turku University Hospital, Turku, Finland (M.O.W.P., K.C., A.T.); Department of Clinical Pharmacology, University of Helsinki, Helsinki, Finland and Individualized Drug Therapy Research Program, Faculty of Medicine, University of Helsinki, Helsinki, Finland (M.Ne., M.Ni., J.T.B.); Department of Regional Health Research, University of Southern Denmark, Esbjerg, Denmark and Department of Clinical Pharmacology, Odense University Hospital, Odense, Denmark (T.K.B.); Department of Clinical Pharmacology, HUS Diagnostic Center, Helsinki University Hospital, Helsinki, Finland (M.Ni., J.T.B.); and Pharmaceutical Sciences Laboratory, Faculty of Science and Engineering, Åbo Akademi University, Turku, Finland (A.M.F.)

Received May 15, 2024; accepted October 3, 2024

ABSTRACT

In vitro evidence shows that the acyl-β-D-glucuronide metabolite of candesartan inhibits cytochrome P450 (CYP) 2C8 with an inhibition constant of 7.12 μM. We investigated the effect of candesartan on the plasma concentrations and glucose-lowering effect of repaglinide, a sensitive clinical CYP2C8 index substrate. In a randomized crossover study, ten healthy volunteers ingested 8 mg of candesartan or placebo daily for three days, and on day 3, they also ingested 0.25 mg of repaglinide one hour after candesartan or placebo. We measured the plasma concentrations of repaglinide, candesartan, and candesartan acyl-β-D-glucuronide, and blood glucose concentrations for up to nine hours after repaglinide intake. Candesartan had no effect on the area under the plasma concentration-time curve and peak plasma concentration of repaglinide compared with placebo, with ratios of geometric means of 1.02 [*P* = 0.809; 90% confidence interval (CI) 0.90–1.15] and 1.13 (*P* = 0.346; 90% CI 0.90–1.43), respectively. Other pharmacokinetic variables and blood glucose concentrations were neither affected. Candesartan acyl-β-D-glucuronide was detectable in seven subjects, in whom the peak concentration of repaglinide was 1.32-fold higher in the candesartan phase than in the placebo phase (*P* = 0.041; 90% CI 1.07–1.62). Systemic concentrations of candesartan acyl-β-D-glucuronide were very low compared with its CYP2C8 inhibition constant (ratio ≪ 0.1). Furthermore, in a cohort of 93 cancer patients, no indication of decreased paclitaxel clearance was found in four patients using candesartan concomitantly. In conclusion, candesartan therapy is unlikely to inhibit CYP2C8-mediated metabolism of other drugs to any clinically significant extent.

SIGNIFICANCE STATEMENT

The findings of this study suggest that candesartan is unlikely to cause drug-drug interactions via inhibition of cytochrome P450 (CYP) 2C8. Although candesartan acyl-β-D-glucuronide has been shown to inhibit CYP2C8 in vitro, it shows no clinically relevant CYP2C8 inhibition in humans due to low systemic concentrations.

Introduction

Candesartan, an angiotensin II receptor inhibitor, is widely used to treat elevated blood pressure and systolic heart failure (Cernes et al., 2011). Administered as the prodrug candesartan cilexetil, active candesartan is formed through hydrolysis during absorption, yielding an absolute bioavailability of 14% for candesartan from the tablet formulation. Peak plasma concentration (C_{max}) is reached approximately four hours after ingestion, and more than 99% of candesartan is protein-bound. Candesartan is excreted into both feces and urine, primarily as candesartan (70–80% of radioactivity), with an elimination half-life of approximately nine hours. In addition, a small proportion is metabolized through O-deethylation and glucuronidation (Kondo et al., 1996a,b; United States Food and Drug Administration, 1998; Alonen et al., 2008a,b; Katsube

This work was supported by State funding for university-level health research (the Hospital District of Southwest Finland, Finland) and the TYKS Foundation (Turku, Finland).

No author has an actual or perceived conflict of interest with the contents of this article.

Part of the results of this work were presented at the Second Nordic Conference on Personalized Medicine in Turku, Finland, from 14 to June 16, 2023, and at the 19th World Congress of Basic & Clinical Pharmacology in Glasgow, United Kingdom, on July 6, 2023.

dx.doi.org/10.1124/dmd.124.001798.

[S] This article has supplemental material available at dmd.aspetjournals.org.

ABBREVIATIONS: AUC, area under the plasma concentration-time curve; AUCR, area under the plasma concentration-time curve ratio; CI, confidence interval; C_{max}, peak plasma concentration; CYP, cytochrome P450; DDI, drug-drug interaction; K_i, inhibition constant; OATP, organic anion-transporting polypeptide; $t_{1/2}$, terminal half-life; t_{max}, time to C_{max}; UGT, uridine 5'-diphospho-glucuronosyltransferase.

et al., 2021). Candesartan has been thought to possess low drug–drug interaction (DDI) potential based on in vitro and in vivo studies (Jonkman et al., 1997; Taavitsainen et al., 2000; Pietruck et al., 2005; Miura et al., 2009; Aberg et al., 2011; Brendel et al., 2013; Senda et al., 2017; Kim et al., 2018; Gundlach et al., 2021).

Previously, the cytochrome P450 (CYP) 2C8 inhibitory potency of candesartan was shown to be relatively low in vitro with a half-maximal inhibitory concentration of 36.2 μM (Walsky et al., 2005). Recently, however, Katsube et al. (2018) found an increased incidence of neutropenia in patients receiving candesartan at a median dose of 8 mg, and the anticancer agent paclitaxel, a CYP2C8 substrate, concomitantly. In a subsequent study, the authors demonstrated that candesartan and its glucuronide metabolites inhibited the CYP2C8 and CYP3A4-mediated hydroxylation of paclitaxel, as well as organic anion-transporting polypeptide (OATP) 1B1 and OATP1B3 in vitro. Of note, the acyl-β-D-glucuronide of candesartan inhibited the CYP2C8-mediated hydroxylation of paclitaxel with a particularly low inhibition constant (K_i) of 7.12 μM. This suggests that candesartan could increase the concentrations of CYP2C8 substrate drugs in humans, which could also explain the observed cases of neutropenia during concomitant treatment with candesartan and paclitaxel (Katsube et al., 2021). In rats and dogs, candesartan acyl-β-D-glucuronide was present in the urine and feces, but it was undetectable in the plasma of rats (Kondo et al., 1996a,b). Recombinant human uridine 5′-diphosphoglucuronosyltransferase (UGT) enzymes as well as human liver microsomes also metabolize candesartan into its acyl-β-D-glucuronide (Alonen et al., 2008a,b), but the presence of this metabolite in humans is not known.

Glucuronide metabolites of drugs have previously been shown to mediate clinically significant DDIs, especially those involving CYP2C8 (Niemi et al., 2003; Shitara et al., 2004; Ogilvie et al., 2006; Tornio et al., 2014, 2022; Backman et al., 2016). For example, clopidogrel increased the plasma concentrations of repaglinide, a clinical index substrate of CYP2C8, up to 5-fold, with clopidogrel acyl-β-D-glucuronide identified as the actual inhibitor according to in vitro data and pharmacokinetic modeling (Tornio et al., 2014). In the current trial, we aimed to investigate the effect of the concomitant administration of candesartan on repaglinide in healthy volunteers. We also measured the plasma concentrations of candesartan acyl-β-D-glucuronide to assess its role in the possible DDI.

Materials and Methods

Subjects and Study Design. Ten healthy nonsmoking volunteers (six men and four women; age range, 19–28 years; body mass index range, 18.9–28.1 kg/m^2) not using any continuous medication, including hormonal contraception, were recruited to the trial. Before inclusion, they gave written informed consent, and their health was confirmed by medical history interview, physical examination, and routine laboratory tests (basic blood count and blood platelets, plasma alanine aminotransferase, plasma alkaline phosphatase, plasma glutamyl transferase, plasma creatinine, estimated glomerular filtration rate, plasma sodium, plasma potassium, and plasma glucose, as well as serum human chorionic gonadotropin for females). All subjects had their plasma creatinine, potassium, and sodium concentrations within reference ranges, as well as their systolic blood pressure at or above 110 mmHg. The study protocol was approved by the Ethics Committee of the Hospital District of Southwest Finland (ETMK 79/2021) and the Finnish Medicines Agency Fimea (EudraCT number 2021-003178-29). The subjects were randomized to ingest either placebo (Placebo 9 mm tablet, University Pharmacy, Helsinki, Finland) or 8 mg of candesartan cilexetil (Atacand 8 mg tablet, Cheplapharm Arzneimittel GmbH, Greifswald, Germany) once daily at 8AM for 3 days per an open-label, two-phase, crossover design. A wash-out period of at least two weeks separated the trial phases. In the morning of day 3, after an overnight fast, the subjects ingested 0.25 mg of repaglinide (prepared as capsules by Tyks Hospital Pharmacy from Repaglinide Krka 0.5 mg tablets, KRKA, d.d., Novo mesto, Slovenia) at 9AM, precisely 1 hour after the final dose of placebo or candesartan. The subjects received a standardized light breakfast 15 minutes after repaglinide ingestion, snacks after 1 and 2 hours, a warm meal after 3 hours, and snacks after 7 and 9 hours. Oral carbohydrates, intramuscular glucagon and intravenous glucose solution were also available but were not needed. Consumption of grapefruit and its juice was prohibited for one week prior to and throughout the trial, and consumption of other drugs was prohibited for one week prior to and during the days of repaglinide administration.

Blood Sampling. On the study days (day 3), blood was sampled from an antebrachial vein through a cannula or needle at our laboratory: before administering placebo or candesartan, as well as 5 minutes before and 15, 30, 45, 60, 80, and 100 minutes after and 2, 2 1/2, 3, 4, 5, 7, and 9 hours after administering repaglinide. Blood samples were collected into EDTA-containing tubes. As a safety measure, glucose concentrations were immediately measured in the whole blood samples using an instant glucose meter (CareSense Dual; I-Sense Inc, Seoul, Korea). Plasma was then separated by centrifugation and stored at -80°C until analysis.

Drug Concentration Measurements. The plasma concentrations of repaglinide, candesartan, and candesartan acyl-β-D-glucuronide were measured in the collected samples using liquid chromatography-tandem mass spectrometry. Reference repaglinide, candesartan, and the corresponding stable isotope-labeled internal standards repaglinide-d_5 and candesartan-d_5 were purchased from Toronto Research Chemicals (North York, ON, Canada). Candesartan acyl-β-D-glucuronide was purchased from SynInnova (Edmonton, AB, Canada). Other reagents and organic solvents were of commercially available analytical grade.

For repaglinide, reference calibration standards and quality control samples were prepared in blank human plasma and processed along with the study samples. The samples were purified using a 96-well Oasis MAX μElution plate (Waters Corporation, Milford, MA, USA) according to the manufacturer's instructions. An aliquot of 100 μl of sample was mixed with 30 μl of 5% phosphoric acid containing the internal standard (5 ng/ml), and the sample mixture was drawn through the preconditioned extraction plate. The plate was then washed with 200 μl of 5% ammonium hydroxide in water, and the compounds were eluted three times with 30 μl of 2.5% formic acid in methanol. The chromatographic separation was performed on a Symmetry C8 column (150 × 2.1 mm internal diameter, particle size 3.5 μm; Waters Corporation, Milford, MA, USA) using a mobile phase of 5 mM ammonium formate, pH 3.6 adjusted with glacial formic acid (channel A) and acetonitrile (channel B). The mobile phase gradient was set as follows: 1 minute at 40% B, a linear ramp to 65% B over 2 minutes, 2 minutes on hold at 65% B, a second linear ramp to 95% over 2 minutes, and 2.5 minutes at 95% B followed by equilibration at 40% B. The flow rate was set at 300 μl/min and the column temperature was maintained at 35°C. Quantification of drug concentrations was carried out using a 5500 QTRAP liquid chromatography-tandem mass spectrometry system with an electrospray ion source (AB Sciex, Toronto, ON, Canada). The mass spectrometer was operated in positive multiple reaction monitoring mode, and the quantification was based on the mass-to-charge (m/z) ion transition m/z 453 → m/z 230 for repaglinide. The lower limit of quantification was 0.01 ng/ml for repaglinide. The between-day precisions (expressed as coefficients of variation) for the quality control samples (0.1 ng/ml and 2 ng/ml) were below 10% and the between-day accuracies were within ± 15% for repaglinide.

For candesartan and candesartan acyl-β-D-glucuronide, reference calibration standards and quality control samples were prepared in blank human plasma and processed along the study samples. The samples were purified using protein precipitation and phospholipid removal. An aliquot of 50 μl of the plasma sample was mixed with 150 μl of the protein precipitation solution containing the internal standard (12 ng/ml) and vortexed for 1 minute. After centrifugation, supernatant aliquots of 100 μl were treated with Ostro Protein Precipitation & Phospholipid Removal Plate (Waters Corporation, Milford, MA, USA). The wells were then washed with 100 μl methanol/water (1:1, v/v) and the solvent was collected into the same well with the previous aliquot. The chromatographic separation was performed on a Kinetex C18 column (100 × 2.1 mm, 2.6 μm; Phenomenex, Inc., Torrance, CA, USA) coupled with a SecurityGuard ULTRA C18 guard column (2.1 × 4 mm; Phenomenex, Inc., Torrance, CA, USA). The mobile phase consisted of 0.1% formic acid in water (channel A) and 0.1% formic acid in acetonitrile (channel B). The mobile phase gradient was as follows: 0.0–0.5 minutes: 30% B in A; 0.5–4.0 minutes: 30–70% B in A (linear gradient); 4.0–4.5 minutes: 70–90% B in A (linear gradient); 4.5–6.0 minutes: 90% B in A; 6.0–6.5 minutes: 90–30% B in A (linear gradient) and 6.5–8.0 minutes: 30% B in A. The flow rate was set at 300 μl/min and column temperature was set at 40°C. Injection volume was 10 μl. Quantification of drug concentrations was carried out using a QTRAP 6500+ liquid chromatography-tandem mass spectrometry system (AB Sciex, Toronto, ON, Canada), using positive Turbo Ion Spray ionization and single reaction monitoring mode. The single reaction monitoring transitions were

m/z 441.2 → *m/z* 263.0 for candesartan, *m/z* 617.2 → *m/z* 441.3 for candesartan acyl-β-D-glucuronide, and *m/z* 446.2 → *m/z* 268.3 for candesartan-d_5 which was the internal standard for both analytes. The lower limit of quantification was 2 ng/ml for candesartan and 1 ng/ml for candesartan acyl-β-D-glucuronide. The interassay precision (as coefficients of variation) for the quality control samples (6 ng/ml, 40 ng/ml and 150 ng/ml for candesartan; 1.5 ng/ml, 7.5 ng/ml and 40 ng/ml for candesartan acyl-β-D-glucuronide) were below 15% for both analytes and interassay accuracies were within ± 15% for both analytes.

Measurement of Unbound Plasma Fraction of Candesartan-Acyl-β-D-Glucuronide. Samples at concentration levels 7.5 ng/ml and 40 ng/ml were prepared by spiking adequate amounts of candesartan acyl-β-D-glucuronide working solutions into analyte-free human K_2EDTA plasma and ultrafiltered analyte-free human K_2EDTA plasma (prepared with Amicon Ultra-15 Centrifugal Filters 30 kDa MWCO, Merck KGaA, Darmstadt, Germany). For sample analysis, 950 μl aliquots of human K_2EDTA plasma or ultrafiltered analyte-free human K_2 EDTA plasma spiked with candesartan acyl-β-D-glucuronide were pipetted into Centrifree Ultrafiltration Centrifugal Filters (30 kDa MWCO, Merck KGaA, Darmstadt, Germany) and centrifuged for 15 minutes at 1900 g until approximately 100 μl of ultrafiltrate was recovered. Thereafter, sample analysis was continued as in the determination of total candesartan and total candesartan acyl-β-D-glucuronide concentrations. The amount of protein-free (unbound) candesartan acyl-β-D-glucuronide was determined as % from the total amount of candesartan acyl-β-D-glucuronide.

Pharmacokinetic Analysis. The areas under the plasma concentration-time curves from zero to nine ($AUC_{0\text{-}9\ hours}$) or ten hours ($AUC_{0\text{-}10\ hours}$) and to infinity ($AUC_{0\text{-}\infty}$), C_{max}, times to peak concentrations (t_{max}), as well as the elimination half-lives ($t_{1/2}$) of repaglinide and candesartan, were calculated using standard noncompartmental analysis with Phoenix WinNonlin version 8.3 (Certara, Princeton, NJ, USA).

Pharmacodynamic Analysis. The safety blood glucose measurements were also treated as a secondary pharmacodynamic outcome measure. The $AUC_{0\text{-}3\ hours}$ and $AUC_{0\text{-}9\ hours}$ of blood glucose were calculated using the trapezoidal method. Baseline, minimum, and maximum concentrations of blood glucose were derived directly from the data, and the mean concentrations from zero to three hours and nine hours were also calculated by dividing $AUC_{0\text{-}3\ hours}$ and $AUC_{0\text{-}9\ hours}$ by 3 hours and 9 hours, respectively.

Static Drug-Drug Interaction Predictions. To predict the overall effect of candesartan and candesartan acyl-β-D-glucuronide on the plasma concentrations of repaglinide via different inhibition mechanisms, the following eq. (1) was used.

$$\mathrm{AUCR} = \frac{1}{\mathrm{A}} \times \frac{1}{\mathrm{B}} \times \frac{1}{\mathrm{C}} \quad (1)$$

where

$$\mathrm{A} = \frac{1 - F_{g,\mathrm{REP}}}{1 + \dfrac{[I]_{g,\mathrm{CAN}}}{K_{i,\mathrm{CYP3A4,CAN}}}} + F_{g,\mathrm{REP}}$$

$$\mathrm{B} = \frac{f_{m,\mathrm{CYP3A4,REP}}}{1 + \dfrac{[I]_{h,\mathrm{CAN}}}{K_{i,\mathrm{CYP3A4,CAN}}} + \dfrac{[I]_{h,\mathrm{GLU}}}{K_{i,\mathrm{CYP3A4,GLU}}}} + \frac{f_{m,\mathrm{CYP2C8,REP}}}{1 + \dfrac{[I]_{h,\mathrm{CAN}}}{K_{i,\mathrm{CYP2C8,CAN}}} + \dfrac{[I]_{h,\mathrm{GLU}}}{K_{i,\mathrm{CYP2C8,GLU}}}} + \left[1 - \left(f_{m,\mathrm{CYP3A4,REP}} + f_{m,\mathrm{CYP2C8,REP}}\right)\right]$$

$$\mathrm{C} = \frac{f_{t,\mathrm{OATP1B1,REP}}}{1 + \dfrac{[I]_{pv,\mathrm{CAN}}}{K_{i,\mathrm{OATP1B1,CAN}}} + \dfrac{[I]_{pv,\mathrm{GLU}}}{K_{i,\mathrm{OATP1B1,GLU}}}} + \left(1 - f_{t,\mathrm{OATP1B1,REP}}\right)$$

AUCR refers to the ratio of the areas under the concentration-time curves of the victim drug in the presence and absence of the perpetrator compounds. Factor A predicts the effect of candesartan (CAN) on the CYP3A4-mediated metabolism of repaglinide (REP) in the gut; factor B predicts the effects of candesartan and candesartan acyl-β-D-glucuronide (GLU) on the CYP2C8- and CYP3A4-mediated metabolism of repaglinide in the liver; and factor C predicts the effects of candesartan and candesartan acyl-β-D-glucuronide on the OATP1B1-mediated transport of repaglinide into the liver. The prediction equation was customized from previously proposed mathematical models (Wang et al., 2004; Ito et al., 2005; Fahmi et al., 2008; Templeton et al., 2008; Zamek-Gliszczynski et al., 2009). Since there is no evidence of time-dependent inhibition or induction of CYP enzymes or transporters by candesartan or candesartan acyl-β-D-glucuronide, only reversible inhibition was included in the equation. F_g expresses the fraction of intact victim drug entering the portal vein; $[I]_g$ depicts the concentration of the perpetrator drug in enterocytes; K_i denotes the inhibition constant of the interaction between the perpetrator and the enzyme or transporter; $[I]_{pv}$ and $[I]_h$ are the unbound concentrations of the perpetrator in the portal vein and liver, respectively; and f_m and f_t express the fraction of the victim drug metabolized and transported by the indicated enzyme or transporter, respectively. The highest

TABLE 1

Pharmacokinetic and biochemical parameters of candesartan, candesartan acyl-β-D-glucuronide, and repaglinide, and physiological parameters used in static drug-drug predictions

Parameter	Value	Reference/comment
Candesartan		
Dose	8 mg (18.16 μmol) or 32 mg (72.64 μmol)[a]	Current trial or highest clinically used dose
F_a	1.00	Worst-case scenario
F_g	1.00	Worst-case scenario
k_a	6.00 1/h[b]	Ito et al., 1998
R_B	0.53[c]	United States Food and Drug Administration, 1998
$f_{u,p}$	0.01[d]	United States Food and Drug Administration, 1998
C_{max} (total)	0.33 or 1.32 μM[e]	Current trial
R_L	1 or 3.8793[f]	Supplemental Methods, Supplemental Table 1
$[I]_g$	6.05 or 24.22 μM[g]	Rostami-Hodjegan and Tucker, 2004
$[I]_{pv}$	0.024 or 0.098 μM[h]	Ito et al., 1998
$[I]_h$	0.024, 0.095, 0.098 or 0.38 μM[i]	
$K_{i,CYP3A4}$	125 μM[j]	Katsube et al., 2021
$K_{i,CYP2C8}$	18.1 μM[k]	Walsky et al., 2005
$K_{i,OATP1B1}$	10.0 μM[l]	Karlgren et al., 2012
Candesartan acyl-β-D-glucuronide		
$f_{u,p}$	0.01[m]	Current trial
C_{max} (total)	0.01 or 0.04 μM[n]	Current trial
R_L	1[f]	Supplemental Methods, Supplemental Table 1
$[I]_{pv}$	0.00009 or 0.0004 μM[o]	
$[I]_h$	0.00009 or 0.0004 μM[i]	
$K_{i,CYP3A4}$	79.50 μM[p]	Katsube et al., 2021
$K_{i,CYP2C8}$	7.12 μM	Katsube et al., 2021
$K_{i,OATP1B1}$	5.00 μM[q]	Katsube et al., 2021
Repaglinide		
F_g	0.89	Gertz et al., 2010
$f_{m,CYP3A4}$	0.16[r]	
$f_{m,CYP2C8}$	0.84	Honkalammi et al., 2011
$f_{t,OATP1B1}$	0.65[s]	Niemi et al., 2005
Physiology		
Q_{en}	18.0 l/h/70 kg	Yang et al., 2007a
Q_h	97.0 l/h/70 kg	Yang et al., 2007b

[a] 8 mg or 32 mg of candesartan; molar mass 440.5 g/mol (National Center for Biotechnology Information, 2023a).
[b] FDA-recommended surrogate value (0.1 1/min).
[c] Ratio of radioactivity in whole blood vs. plasma.
[d] Actually 0.0016.
[e] 145.0 ng/ml at 8 mg dose (highest measured C_{max} in the current trial) and 580.0 ng/ml (linearly scaled) at 32 mg dose; molar mass 440.5 g/mol (National Center for Biotechnology Information, 2023a).
[f] Ratio of concentration in the liver vs. plasma.
[g] $[I]_g = F_a \times k_a \times \mathrm{Dose}/Q_{en}$.
[h] $[I]_{pv} = f_{u,p} \times [C_{max} + (F_a \times F_g \times k_a \times \mathrm{Dose})/Q_h/R_B]$.
[i] $[I]_h = R_L \times [I]_{pv}$.
[j] $IC_{50} > 250$ μM; approximated worst-case scenario $K_i \approx 250$ μM/2 ≈ 125 μM.
[k] $IC_{50} = 36.2$ μM at $K_{m,substrate}$, hence $K_i \approx 36.2$ μM/2 ≈ 18.1 μM.
[l] 52.1% inhibition at $C_{candesartan} = 20$ μM, hence $IC_{50} \approx 20$ μM and $K_i \approx 20$ μM/2 ≈ 10 μM.
[m] Actually 0.0099.
[n] 5.4 ng/ml at 8 mg dose (highest measured C_{max} in the current trial) and 21.6 ng/ml (linearly scaled) at 32 mg; molar mass 616.6 g/mol (National Center for Biotechnology Information, 2023b).
[o] $[I]_{pv} = f_{u,p} \times C_{max}$.
[p] $IC_{50} = 159$ μM, hence $K_i \approx 159$ μM/2 ≈ 79.5 μM.
[q] 40% inhibition at $C_{glucuronide} = 20$ μM, hence $IC_{50} \approx 10$ μM and $K_i \approx 10$ μM/2 ≈ 5 μM.
[r] Assuming CYP3A4 metabolizes the fraction that CYP2C8 does not.
[s] Repaglinide AUC 2.88-fold higher in subjects with *SLCO1B1* 521CC *vs.*521TT genotype (Niemi et al., 2005), and AUCR = 1/(1 − f_t) ↔ f_t = 1 − (1/AUCR) (Zamek-Gliszczynski et al., 2009).

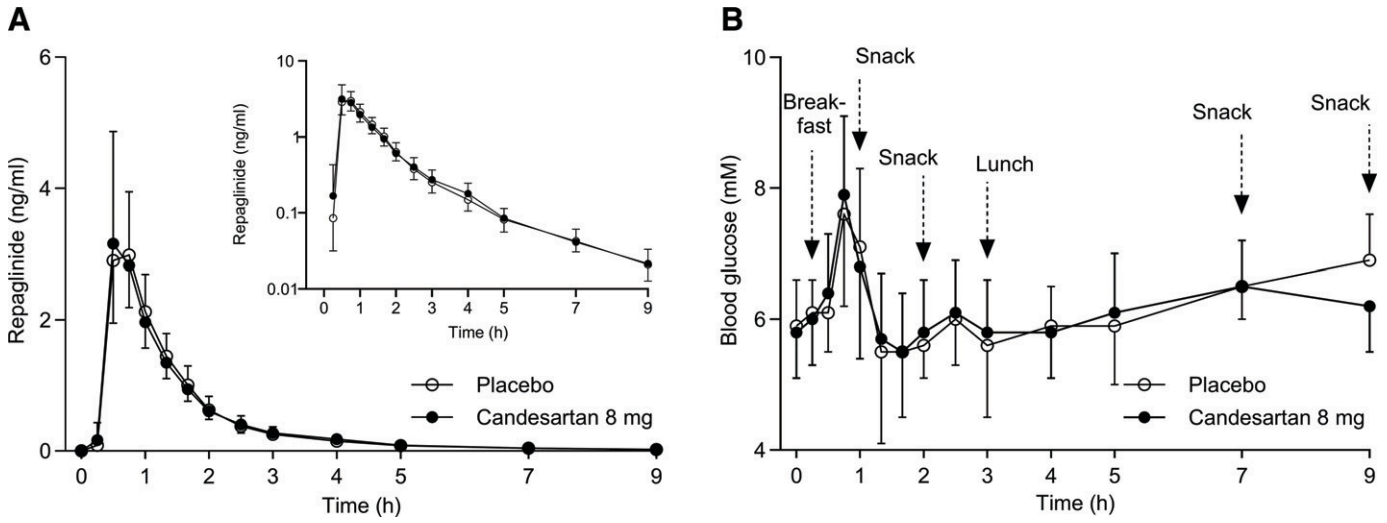

Fig. 1. The effect of candesartan on the plasma concentrations of repaglinide (A) and blood glucose concentrations (B). Ten healthy volunteers ingested 8 mg of candesartan or placebo once daily for three days. On day 3, the subjects ingested 0.25 mg of repaglinide one hour after the day's candesartan or placebo dose. The ingestion of repaglinide marks time zero. (A) Data are presented as geometric means with 90% confidence intervals. The inset is a presentation of the same data on a semilogarithmic scale. Some error bars have been omitted for clarity. (B) Data are presented as arithmetic means with standard deviations. Some error bars have been omitted for clarity.

individual plasma concentrations of candesartan and candesartan acyl-β-D-glucuronide measured in the present trial were used, while the other parameters were derived from literature (Table 1). Four scenarios were predicted: with the currently measured concentrations, and with these concentrations linearly scaled up according to the largest 32 mg clinical dose of candesartan, and assuming liver-to-plasma ratios of either 1 or worst-case scenario (Supplemental Table 1), for candesartan and candesartan acyl-β-D-glucuronide.

Paclitaxel Clearance in a Cancer Patient Cohort. To evaluate the effect of candesartan on paclitaxel pharmacokinetics, we identified candesartan users in a previously described population pharmacokinetic study (Bergmann et al., 2011). The data contained individual clearance values of unbound paclitaxel estimated in 93 women (median age, 60 years) with ovarian cancer treated with 175 mg/m^2 of paclitaxel as a three-hour infusion. Candesartan users were identified by reviewing the recorded concomitant medications of the patients. The previously reported single clopidogrel (a known CYP2C8 inhibitor) user was also identified (Bergmann et al., 2016). Patients not using candesartan, clopidogrel, or any known CYP2C8 inhibitors were designated as the control group.

Statistical Analysis. It was estimated that ten subjects would be sufficient to demonstrate a change of more than 30% in the $AUC_{0\text{-}\infty}$ of repaglinide between the placebo and candesartan phases, with a statistical power of more than 80%. Pharmacokinetic results are expressed as geometric means with geometric coefficients of variation, and as ratios of geometric means with 90% confidence intervals (CIs), except for t_{max} for which median with range is given. Except for t_{max}, pharmacokinetic data were transformed into natural logarithms for statistical testing. Blood glucose results are presented as arithmetic means with standard deviations. Estimated paclitaxel clearance values from the patient cohort are presented as scatter plots, with median and interquartile range reported for the patients not using candesartan or clopidogrel. Paired t test or Wilcoxon signed-rank test was used to test the statistical significances of differences between the pharmacokinetic trial phases. A P-value below 0.05 was considered statistically significant. All statistical tests were performed with JMP Pro version 17 (SAS Institute, Cary, NC, USA).

Results

Effect of Candesartan on Repaglinide. Compared with placebo, candesartan had no relevant effect on any of the pharmacokinetic or pharmacodynamic variables of repaglinide (Figs. 1 and 2, Table 2). The geometric mean ratios of the $AUC_{0\text{-}\infty}$ and C_{max} of repaglinide in the candesartan phase compared with the placebo phase were 1.02 (P = 0.809; 90% CI 0.90–1.15) and 1.13 (P = 0.346; 90% CI 0.90–1.43), respectively. There were no differences in the maximum blood glucose concentrations nor in the mean blood glucose concentrations between the candesartan and placebo phases. However, the minimum blood glucose concentration was slightly higher in the candesartan phase than in the placebo phase (P = 0.020; 4.9 mM, S.D. ± 0.6 mM, vs. 4.5 mM, S.D. ± 0.5 mM).

Plasma Concentrations of Candesartan and Candesartan Acyl-β-D-Glucuronide. On the day of repaglinide administration, the geometric mean of candesartan C_{max} was 59.8 ng/ml (range 34.2–145 ng/ml; Fig. 3A, Table 3). There was also considerable interindividual variation

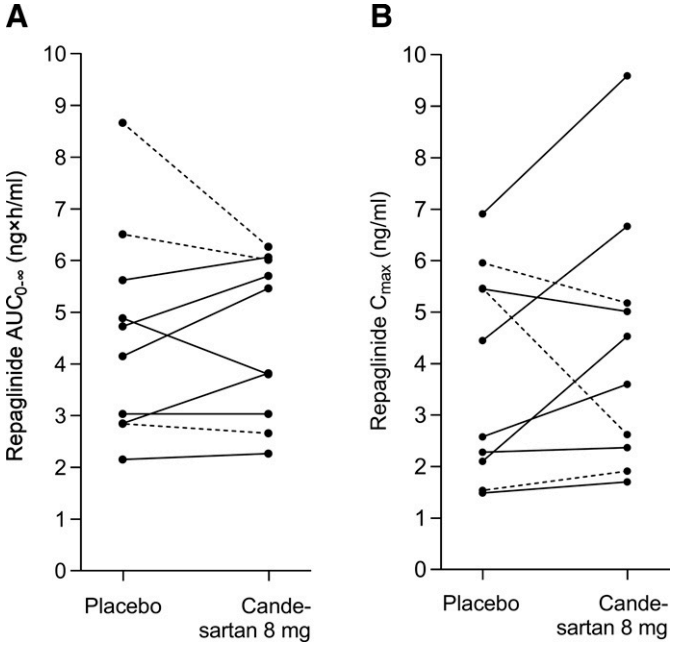

Fig. 2. The effect of candesartan on the individual areas under the plasma concentration-time curves ($AUC_{0\text{-}\infty}$) (A) and peak concentrations (C_{max}) (B) of repaglinide. Ten healthy volunteers ingested 8 mg of candesartan or placebo once daily for three days. On day 3, the subjects ingested 0.25 mg of repaglinide one hour after the day's candesartan or placebo dose. The connected dots represent individual values in the placebo and candesartan phases, respectively. The solid lines indicate subjects with at least one quantifiable (≥1.00 ng/ml) candesartan acyl-β-D-glucuronide plasma concentration measurement, whereas the dashed lines indicate subjects below that limit.

TABLE 2

Pharmacokinetic variables of repaglinide and blood glucose variables in ten healthy volunteers following three days of daily doses of placebo or 8 mg of candesartan, and a single 0.25 mg dose of repaglinide one hour after placebo or candesartan on day 3. Pharmacokinetic values are expressed as geometric means with geometric coefficients of variation, except for t_{max}, for which median with range is given. Blood glucose values are expressed as arithmetic means with standard deviations. Pharmacokinetic data, except for t_{max}, were logarithmically transformed for statistical testing. Paired *t* test was applied on pharmacokinetic and blood glucose data, except for Wilcoxon signed rank test for t_{max}

Variable	Placebo	Candesartan 8 mg	Ratio (90% CI)	*P* value
Repaglinide				
C_{max} (ng/ml)	3.30 (60.3)	3.75 (57.5)	1.13 (0.90; 1.43)	0.346
t_{max} (h)	0.50 (0.50–0.75)	0.50 (0.50–1.33)	N/A	>0.999
$t_{1/2}$ (h)	1.24 (15.1)	1.27 (12.4)	1.02 (0.93; 1.13)	0.691
$AUC_{0\text{-}9\ h}$ (ng*h/ml)	4.15 (42.8)	4.21 (36.9)	1.02 (0.90; 1.15)	0.821
$AUC_{0\text{-}\infty}$ (ng*h/ml)	4.18 (43.0)	4.24 (37.3)	1.02 (0.90; 1.15)	0.809
Blood glucose				
Baseline concentration (mM)	5.9 (0.7)	5.8 (0.7)	N/A	0.748
Minimum concentration (mM)	4.5 (0.5)	4.9 (0.6)	N/A	0.020*
Maximum concentration (mM)	8.1 (1.0)	8.1 (1.1)	N/A	0.959
Mean concentration from 0 to 3 h (mM)	6.1 (0.5)	6.1 (0.6)	N/A	0.704
Mean concentration from 0 to 9 h (mM)	6.2 (0.4)	6.2 (0.4)	N/A	0.923

N/A, not applicable.
* $P < 0.05$ vs. placebo phase.

in the plasma concentrations of candesartan acyl-β-D-glucuronide. With a lower limit of quantification of 1.00 ng/ml, candesartan acyl-β-D-glucuronide was quantifiable in the plasma of 7 out of 10 subjects, with the highest measurement in any subject reaching 5.4 ng/ml (Fig. 3B). The unbound fraction of candesartan acyl-β-D-glucuronide in plasma was 0.99%. Due to low plasma concentrations, we were unable to calculate the pharmacokinetic parameters of candesartan acyl-β-D-glucuronide.

Predicted Effects of Candesartan on Repaglinide Plasma Concentrations Based on In Vitro Data. The prediction eq. (1) indicated no clinically significant inhibition of CYP2C8, CYP3A4, or OATP1B1 by candesartan or candesartan acyl-β-D-glucuronide, even in the worst-case scenario at a 32 mg candesartan dose (Table 4). Thus, the static predictions were in agreement with the observation of no significant effect of candesartan on the plasma concentrations of repaglinide.

Pharmacokinetics of Repaglinide in Subjects with Quantifiable Candesartan Acyl-β-D-Glucuronide Plasma Concentrations. A post hoc analysis revealed that the C_{max} of repaglinide was 1.32-fold higher ($P = 0.041$; 90% CI 1.07–1.62) in the candesartan phase compared with placebo phase in the subset of the seven subjects who had quantifiable candesartan acyl-β-D-glucuronide concentrations in plasma. With the exception of one individual, the C_{max} of repaglinide was greater in the candesartan phase than in the placebo phase in these subjects (Fig. 2). However, we found no statistically significant differences in other pharmacokinetic or pharmacodynamic variables of repaglinide (data not shown).

Estimated Clearance of Unbound Paclitaxel in Ovarian Cancer Patients with Concomitant Perpetrators. In patients not using candesartan or clopidogrel, the median of estimated unbound paclitaxel clearance values was 383.12 l/h (interquartile range 329.65–450.50 l/h) (Fig. 4). Four patients were using candesartan, specifically Atacand 16 mg (candesartan cilexetil), Atacand at an unrecorded dose, Atacand Zid (candesartan cilexetil and hydrochlorothiazide) at unrecorded doses, and Atazid 8 mg/12.5 mg (8 mg of candesartan cilexetil and 12.5 mg of hydrochlorothiazide). The estimated unbound paclitaxel clearance values in these candesartan users were 469.98 l/h, 641.41 l/h, 317.22 l/h, and 331.72 l/h, respectively. As previously described, one patient was using clopidogrel and presented with the second lowest paclitaxel clearance in the cohort (Bergmann et al., 2016).

Discussion

In the present study, typical therapeutic doses of candesartan had no clinically meaningful effect on the plasma concentrations of repaglinide in healthy volunteers. The $AUC_{0\text{-}\infty}$, C_{max}, and $t_{1/2}$ of repaglinide remained practically unchanged in the candesartan phase compared with the placebo phase. Our static prediction results are in line with these

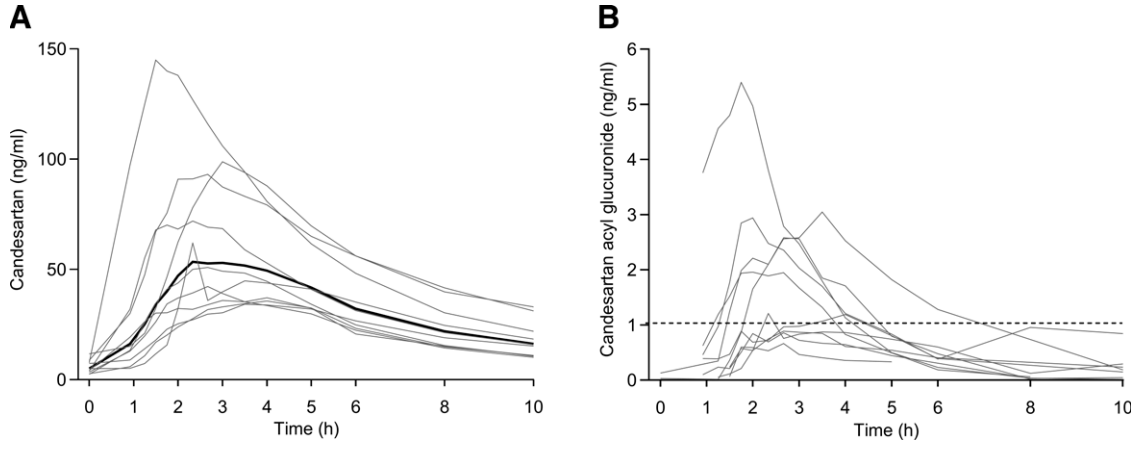

Fig. 3. Individual plasma concentrations of candesartan (A) and candesartan acyl-β-D-glucuronide (B) in ten healthy volunteers on the third day of 8 mg of candesartan once daily. (A) The bold curve indicates the geometric means of individual values. (B) The dashed horizontal line indicates the lower limit of quantification for candesartan acyl-β-D-glucuronide.

TABLE 3

Pharmacokinetic variables of candesartan in ten healthy volunteers following three days of ingesting daily 8 mg doses of candesartan. Values are expressed as geometric means with geometric coefficients of variation, except for t_{max}, for which median with range is given

C_{max} (ng/ml)	59.78 (49.84)
t_{max} (h)	2.67 (1.50–4.00)
$t_{1/2}$ (h)	3.69 (18.67)
$AUC_{0\text{-}10\ h}$ (ng*h/ml)	329.64 (42.49)
$AUC_{0\text{-}\infty}$ (ng*h/ml)	418.64 (42.75)

findings, indicating minimal effect of candesartan on the plasma concentrations of repaglinide even at the highest clinically approved candesartan doses.

We used the antidiabetic agent repaglinide as a clinical index substrate of CYP2C8. Repaglinide is extensively and rapidly metabolized to a number of phase I metabolites, including the aromatic amine M1 and dicarboxylic acid M2 mainly formed by CYP3A4, and the piperidine-hydroxylated M4 and isopropyl-hydroxylated M0-OH primarily formed by CYP2C8 (Guay, 1998; Bidstrup et al., 2003). It has been estimated that up to 84% of repaglinide is metabolized by CYP2C8, and its sensitivity to CYP2C8 inhibitors makes it a recommended clinical index substrate of CYP2C8 (Honkalammi et al., 2011; Tornio et al., 2014, 2019; United States Food and Drug Administration, 2023). However, repaglinide is also transported by OATP1B1, which may have clinical implications (Niemi et al., 2005; Honkalammi et al., 2011). Therefore, along with CYP2C8, OATP1B1 and CYP3A4 can also play a role in DDIs of repaglinide.

In their in vitro assays with recombinant CYP enzymes, Katsube et al. (2021) showed that candesartan, candesartan *N*2-glucuronide, and candesartan acyl-β-D-glucuronide all inhibited the CYP2C8- and CYP3A4-mediated hydroxylation of paclitaxel, and the OATP1B1-mediated transport of 2',7'-dichlorofluorescein. The strongest observed effect was the reversible inhibition of CYP2C8 by candesartan acyl-β-D-glucuronide (K_i 7,120 nM). The authors suggested that this mechanism could be the underlying cause of the high incidence of severe neutropenia previously observed in patients receiving candesartan and paclitaxel (Katsube et al., 2018, 2021). In the current trial, however, we did not observe any clinically significant DDI between candesartan and repaglinide. Compliance of the subjects to candesartan was confirmed with trough concentration measurements and controlled administration of the last candesartan dose on the days of repaglinide ingestion. Moreover, despite a small number of candesartan users, real-world paclitaxel clearance data from a patient cohort offers no support for a pharmacokinetic DDI between candesartan and paclitaxel. Thus, inhibition of CYP2C8 is unlikely to explain the previously suggested DDI between candesartan and paclitaxel, either. Further work is required to unveil the mechanisms predisposing some patients to severe paclitaxel-induced neutropenia.

There is an increasing awareness of the involvement of drug metabolites in pharmacokinetic DDIs (Isoherranen et al., 2009; VandenBrink and Isoherranen, 2010; Yeung et al., 2011; European Medicines Agency, 2012; United States Food and Drug Administration, 2020). Several glucuronide metabolites inhibit CYP2C8, which is well illustrated by the drug interactions of gemfibrozil and clopidogrel (Backman et al., 2016). In early studies, the concomitant administration of gemfibrozil increased the $AUC_{0\text{-}\infty}$ of cerivastatin almost 6-fold and that of repaglinide approximately 8-fold (Backman et al., 2002; Niemi et al., 2003). Subsequently, it was found that the 1-*O*-β-glucuronide metabolite of gemfibrozil is a strong, metabolism-based inhibitor of CYP2C8 in vitro (Shitara et al., 2004; Ogilvie et al., 2006). Later, it was found that clopidogrel increased the $AUC_{0\text{-}\infty}$ of repaglinide up to 5-fold in healthy volunteers. In vitro experiments revealed that clopidogrel acyl-β-D-glucuronide, like gemfibrozil 1-*O*-β-glucuronide, is an irreversible mechanism-based inhibitor of CYP2C8. This was the most important mechanism of the clinical interaction according to physiologically based pharmacokinetic modeling (Tornio et al., 2014). This contrasts with the reversible CYP2C8 inhibition of candesartan acyl-β-D-glucuronide which was not associated with increased repaglinide plasma concentrations in the present study. Of note, recent studies indicate that, apart from CYP2C8, glucuronide metabolites can cause time-dependent inhibition of other CYP enzymes as well (Kahma et al., 2024).

The circulating plasma concentrations [*I*] of candesartan acyl-β-D-glucuronide were found to be several orders of magnitude lower than those of gemfibrozil 1-*O*-β-glucuronide and clopidogrel acyl-β-D-glucuronide, which might also contribute to the different DDI potential. To compare, the mean steady state C_{max} of gemfibrozil 1-*O*-β-glucuronide is approximately 14,500 ng/ml (~34,000 nM) (Itkonen et al., 2019), and that of clopidogrel acyl-β-D-glucuronide approximately 730 ng/ml (~1,500 nM) (Tornio et al., 2014). In contrast, the highest measured concentration of candesartan acyl-β-D-glucuronide was only 5.4 ng/ml (8.8 nM) in the present trial. Thus, the low $[I]/K_i$ ratio $\ll$ 0.1 of candesartan acyl-β-D-glucuronide and its competitive inhibition mechanism are likely to result in only weak and transient CYP2C8-inhibiting effect. Our clinical data are limited to one candesartan dose level only, but

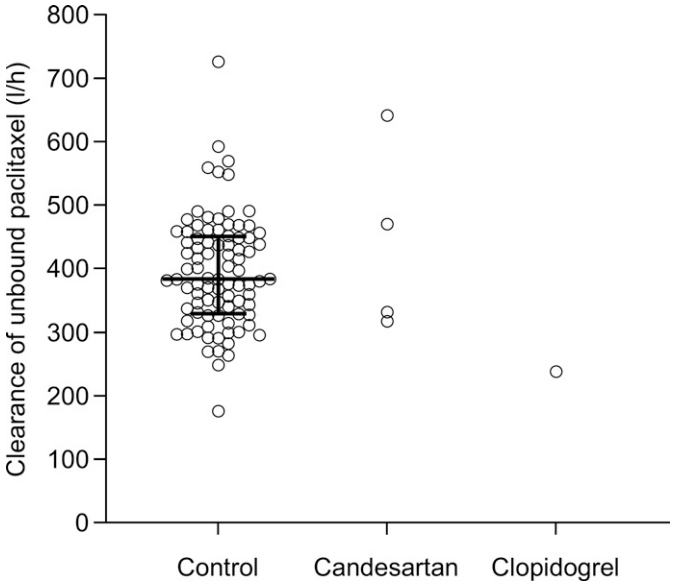

Fig. 4. Estimated individual clearance values of unbound paclitaxel in a cohort of 93 ovarian cancer patients using and not using candesartan or clopidogrel concomitantly. The patients were treated with 175 mg/m^2 of paclitaxel as a three-hour infusion. Four patients were using candesartan, and a single patient was using clopidogrel concomitantly; control patients were not using candesartan, clopidogrel, or any known CYP2C8 inhibitors. The horizontal line indicates median, and the whiskers indicate interquartile range in control patients.

TABLE 4

Predicted ratios of the areas under the plasma concentration-time curves of repaglinide in the presence and absence of candesartan and candesartan acyl-β-D-glucuronide at two different candesartan doses, with liver-to-plasma ratios (R_L) of either 1 or worst-case scenario for candesartan and candesartan acyl-β-D-glucuronide (Supplemental Data)

Candesartan dose	Candesartan R_L = 1; Candesartan acyl-β-D-glucuronide R_L = 1	Candesartan R_L = 3.8793; Candesartan acyl-β-D-glucuronide R_L = 1
8 mg	1.008	1.011
32 mg	1.030	1.043

since the pharmacokinetics of candesartan are linearly dose-proportional in the range of 2–64 mg (United States Food and Drug Administration, 1998), we scaled up our plasma concentration data to predict the effect of the maximum 32 mg clinical dose to simulate the worst-case scenario. Our static DDI predictions offer little support for clinically meaningful CYP2C8 inhibition by candesartan or candesartan acyl-β-D-glucuronide at any clinical dose. Even at the 32 mg dose and corresponding plasma and liver concentrations of candesartan and candesartan acyl-β-D-glucuronide, the predicted effect on repaglinide plasma concentrations was negligible (AUCR = 1.04). It should be noted, as Katsube et al. (2021) also speculated, that the circulating systemic concentrations of candesartan acyl-β-D-glucuronide do not necessarily accurately reflect those in the portal vein and liver, which causes uncertainty in in vitro-to-in vivo extrapolations. However, we predicted the liver-to-plasma ratios of candesartan and candesartan-acyl-β-D-glucuronide and used the highest predicted hepatic concentrations in our prediction equation.

Interestingly, we found that candesartan increased the C_{max} of repaglinide by 32% in those seven subjects with quantifiable candesartan acyl-β-D-glucuronide plasma concentrations. This suggests that in some individuals, candesartan acyl-β-D-glucuronide might indeed inhibit CYP2C8 weakly. According to in vitro studies, candesartan is conjugated to its acyl-β-D-glucuronide by UGT1A7, UGT1A8, UGT1A9, UGT1A10, and UGT2B7 (Alonen et al., 2008b; Katsube et al., 2021). The activities of these UGT enzymes are subject to genetic variation with potentially clinically significant implications (Stingl et al., 2014). While several UGT enzymes can contribute to the glucuronidation of candesartan, genetic variability in UGT activity might produce variability in the systemic concentrations of candesartan acyl-β-D-glucuronide and consequently in the susceptibility to CYP2C8-mediated DDIs. Moreover, inflammatory disease states, including cancer, have been linked with altered pharmacokinetics of various drugs consistent with reduced CYP enzyme and transporter activity (Gatti and Pea, 2022), further predisposing certain individuals to DDIs. However, since the $AUC_{0-\infty}$ of repaglinide remained unaffected even in the subjects with quantifiable candesartan acyl-β-D-glucuronide plasma concentrations, and no decrease in paclitaxel clearance was evident in any of the ovarian cancer patients using candesartan, the potential for clinically meaningful DDIs still appears to be low.

In conclusion, the coadministration of candesartan has no clinically relevant effect on the plasma concentrations or hypoglycemic effect of the CYP2C8 substrate repaglinide. We confirmed the presence of candesartan acyl-β-D-glucuronide in human plasma but, considering its low systemic concentrations and reversible mechanism of CYP2C8 inhibition, its potential to inhibit CYP2C8 to a clinically relevant degree appears low. Therefore, candesartan therapy is unlikely to cause pharmacokinetic DDIs via inhibition of CYP2C8.

Acknowledgments

The authors thank Marika Iljamo, Tiina Ceder, and Karla Saukkonen for their technical assistance.

Data Availability

The individual data supporting the findings of this study cannot be made publicly available to protect the privacy of the study subjects in accordance with legal and ethical requirements.

Authorship Contributions

Participated in research design: Piha, Cajanus, Niemi, Backman, Filppula, Tornio.

Conducted experiments: Piha, Cajanus, Engström, Neuvonen, Tornio.

Performed data analysis: Piha, Filppula, Tornio.

Wrote or contributed to the writing of the manuscript: Piha, Cajanus, Engström, Neuvonen, Bergmann, Niemi, Backman, Filppula, Tornio.

References

Aberg JG, Olofsson B, and Karlson BW (2011) Pharmacokinetic interaction study with fixed high dose combinations of candesartan cilexetil and hydrochlorothiazide. *Int J Clin Pharmacol Ther* **49**:750–755.

Alonen A, Jansson J, Kallonen S, Kiriazis A, Aitio O, Finel M, and Kostiainen R (2008a) Enzyme-assisted synthesis and structure characterization of glucuronic acid conjugates of losartan, candesartan, and zolarsartan. *Bioorg Chem* **36**:148–155.

Alonen A, Finel M, and Kostiainen R (2008b) The human UDP-glucuronosyltransferase UGT1A3 is highly selective towards N2 in the tetrazole ring of losartan, candesartan, and zolarsartan. *Biochem Pharmacol* **76**:763–772.

Backman JT, Filppula AM, Niemi M, and Neuvonen PJ (2016) Role of Cytochrome P450 2C8 in Drug Metabolism and Interactions. *Pharmacol Rev* **68**:168–241.

Backman JT, Kyrklund C, Neuvonen M, and Neuvonen PJ (2002) Gemfibrozil greatly increases plasma concentrations of cerivastatin. *Clin Pharmacol Ther* **72**:685–691.

Bergmann TK, Brasch-Andersen C, Gréen H, Mirza M, Pedersen RS, Nielsen F, Skougaard K, Wihl J, Keldsen N, Damkier P, et al. (2011) Impact of CYP2C8*3 on paclitaxel clearance: a population pharmacokinetic and pharmacogenomic study in 93 patients with ovarian cancer. *Pharmacogenomics J* **11**:113–120.

Bergmann TK, Filppula AM, Launiainen T, Nielsen F, Backman JT, and Brosen K (2016) Neurotoxicity and low paclitaxel clearance associated with concomitant clopidogrel therapy in a 60-year-old Caucasian woman with ovarian carcinoma. *Br J Clin Pharmacol* **81**:313–315.

Bidstrup TB, Bjørnsdottir I, Sidelmann UG, Thomsen MS, and Hansen KT (2003) CYP2C8 and CYP3A4 are the principal enzymes involved in the human in vitro biotransformation of the insulin secretagogue repaglinide. *Brit J Clinical Pharma* **56**:305–314.

Brendel E, Weimann B, Dietrich H, Froede C, and Thomas D (2013) Investigation of bioequivalence of a new fixed-dose combination of nifedipine and candesartan with the corresponding loose combination as well as the drug-drug interaction potential between both drugs under fasting conditions. *CP* **51**:753–762.

Cernes R, Mashavi M, and Zimlichman R (2011) Differential clinical profile of candesartan compared to other angiotensin blockers. *Vasc Health Risk Manag* **7**:749–759.

European Medicines Agency, Committee for Human Medicinal Products (2012) Guideline on the investigation of drug interactions (CPMP/EWP/560/95/Rev. 1 Corr. 2**).

Fahmi OA, Maurer TS, Kish M, Cardenas E, Boldt S, and Nettleton D (2008) A combined model for predicting CYP3A4 clinical net drug-drug interaction based on CYP3A4 inhibition, inactivation, and induction determined in vitro. *Drug Metab Dispos* **36**:1698–1708.

Gatti M and Pea F (2022) The Cytokine Release Syndrome and/or the Proinflammatory Cytokines as Underlying Mechanisms of Downregulation of Drug Metabolism and Drug Transport: A Systematic Review of the Clinical Pharmacokinetics of Victim Drugs of this Drug-Disease Interaction under Different Clinical Conditions. *Clin Pharmacokinet* **61**:1519–1544.

Gertz M, Harrison A, Houston JB, and Galetin A (2010) Prediction of human intestinal first-pass metabolism of 25 CYP3A substrates from in vitro clearance and permeability data. *Drug Metab Dispos* **38**:1147–1158.

Guay DRP (1998) Repaglinide, A Novel, Short-Acting Hypoglycemic Agent for Type 2 Diabetes Mellitus. *Pharmacotherapy* **18**:1195–1204.

Gundlach K, Wolf K, Salem I, Randerath O, and Seiler D (2021) Safety of Candesartan, Amlodipine, and Atorvastatin in Combination: Interaction Study in Healthy Subjects. *Clin Pharmacol Drug Dev* **10**:190–197.

Honkalammi J, Niemi M, Neuvonen PJ, and Backman JT (2011) Dose-Dependent Interaction between Gemfibrozil and Repaglinide in Humans: Strong Inhibition of CYP2C8 with Subtherapeutic Gemfibrozil Doses. *Drug Metab Dispos* **39**:1977–1986.

Isoherranen N, Hachad H, Yeung CK, and Levy RH (2009) Qualitative analysis of the role of metabolites in inhibitory drug-drug interactions: literature evaluation based on the metabolism and transport drug interaction database. *Chem Res Toxicol* **22**:294–298.

Itkonen MK, Tornio A, Neuvonen M, Neuvonen PJ, Niemi M, and Backman JT (2019) Clopidogrel and Gemfibrozil Strongly Inhibit the CYP2C8-Dependent Formation of 3-Hydroxydesloratadine and Increase Desloratadine Exposure In Humans. *Drug Metab Dispos* **47**:377–385.

Ito K, Hallifax D, Obach RS, and Houston JB (2005) Impact of Parallel Pathways of Drug Elimination and Multiple Cytochrome P450 Involvement on Drug-Drug Interactions: CYP2D6 Paradigm. *Drug Metab Dispos* **33**:837–844.

Ito K, Iwatsubo T, Kanamitsu S, Ueda K, Suzuki H, and Sugiyama Y (1998) Prediction of pharmacokinetic alterations caused by drug-drug interactions: metabolic interaction in the liver. *Pharmacol Rev* **50**:387–412.

Jonkman JH, van Lier JJ, van Heiningen PN, Lins R, Sennewald R, and Högemann A (1997) Pharmacokinetic drug interaction studies with candesartan cilexetil. *J Hum Hypertens* **11 Suppl 2**:SupplS31–35.

Kahma H, Paludetto M-N, Neuvonen M, Kurkela M, Filppula AM, Niemi M, and Backman JT (2024) Screening of 16 major drug glucuronides for time-dependent inhibition of nine drug-metabolizing CYP enzymes - detailed studies on CYP3A inhibitors. *Eur J Pharm Sci* **198**:106735.

Karlgren M, Ahlin G, Bergström CAS, Svensson R, Palm J, and Artursson P (2012) In vitro and in silico strategies to identify OATP1B1 inhibitors and predict clinical drug-drug interactions. *Pharm Res* **29**:411–426.

Katsube Y, Hira D, Tsujimoto M, Koide H, Minegaki T, Ikeda Y, Morita S-Y, Nishiguchi K, and Terada T (2018) Concomitant administration of candesartan cilexetil in patients on paclitaxel and carboplatin combination therapy increases risk of severe neutropenia. *Int J Clin Pharmacol Ther* **56**:328–336.

Katsube Y, Tsujimoto M, Koide H, Hira D, Ikeda Y, Minegaki T, Morita S-Y, Terada T, and Nishiguchi K (2021) In Vitro Evidence of Potential Interactions between CYP2C8 and Candesartan Acyl-β-D-glucuronide in the Liver. *Drug Metab Dispos* **49**:289–297.

Kim J-R, Kim S, Huh W, and Ko J-W (2018) No pharmacokinetic interactions between candesartan and amlodipine following multiple oral administrations in healthy subjects. *Drug Des Devel Ther* **12**:2475–2483.

Kondo T, Yoshida K, Yoshimura Y, Motohashi M, and Tanayama S (1996a) Disposition of the new angiotensin II receptor antagonist candesartan cilexetil in rats and dogs. *Arzneimittelforschung* **46**:594–600.

Kondo T, Yoshida K, Yoshimura Y, Motohashi M, and Tanayama S (1996b) Characterization of Conjugated Metabolites of a New Angiotensin II Receptor Antagonist, Candesartan Cilexetil, in Rats by Liquid Chromatography/Electrospray Tandem Mass Spectrometry Following Chemical Derivatization. *J Mass Spectrom* **31**:873–878.

Miura M, Satoh S, Kagaya H, Saito M, Inoue T, Ohkubo T, Habuchi T, and Suzuki T (2009) Effect of telmisartan, valsartan and candesartan on mycophenolate mofetil pharmacokinetics in Japanese renal transplant recipients. *J Clin Pharm Ther* **34**:683–692.

National Center for Biotechnology Information (2023a) PubChem Compound Summary for CID 2541, Candesartan.

National Center for Biotechnology Information (2023b) PubChem Compound Summary for CID 131769984, Candesartan O-glucuronide.

Niemi M, Backman JT, Kajosaari LI, Leathart JB, Neuvonen M, Daly AK, Eichelbaum M, Kivistö KT, and Neuvonen PJ (2005) Polymorphic organic anion transporting polypeptide 1B1 is a major determinant of repaglinide pharmacokinetics. *Clin Pharmacol Ther* **77**:468–478.

Niemi M, Backman JT, Neuvonen M, and Neuvonen PJ (2003) Effects of gemfibrozil, itraconazole, and their combination on the pharmacokinetics and pharmacodynamics of repaglinide: potentially hazardous interaction between gemfibrozil and repaglinide. *Diabetologia* **46**: 347–351.

Ogilvie BW, Zhang D, Li W, Rodrigues AD, Gipson AE, Holsapple J, Toren P, and Parkinson A (2006) Glucuronidation converts gemfibrozil to a potent, metabolism-dependent inhibitor of CYP2C8: implications for drug-drug interactions. *Drug Metab Dispos* **34**:191–197.

Pietruck F, Kiel G, Birkel M, Stahlheber-Dilg B, and Philipp T (2005) Evaluation of the effect of candesartan cilexetil on the steady-state pharmacokinetics of tacrolimus in renal transplant patients. *Biopharm Drug Dispos* **26**:135–141.

Rostami-Hodjegan A and Tucker G (2004) 'In silico' simulations to assess the 'in vivo' consequences of 'in vitro' metabolic drug-drug interactions. *Drug Discov Today Technol* **1**:441–448.

Senda A, Mukai Y, Hayakawa T, Kato Y, Eliasson E, Rane A, Toda T, and Inotsume N (2017) Angiotensin II Receptor Blockers Inhibit the Generation of Epoxyeicosatrienoic Acid from Arachidonic Acid in Recombinant CYP2C9, CYP2J2 and Human Liver Microsomes. *Basic Clin Pharma Tox* **121**:239–245.

Shitara Y, Hirano M, Sato H, and Sugiyama Y (2004) Gemfibrozil and its glucuronide inhibit the organic anion transporting polypeptide 2 (OATP2/OATP1B1:SLC21A6)-mediated hepatic uptake and CYP2C8-mediated metabolism of cerivastatin: analysis of the mechanism of the clinically relevant drug-drug interaction between cerivastatin and gemfibrozil. *J Pharmacol Exp Ther* **311**:228–236.

Stingl JC, Bartels H, Viviani R, Lehmann ML, and Brockmöller J (2014) Relevance of UDP-glucuronosyltransferase polymorphisms for drug dosing: A quantitative systematic review. *Pharmacol Ther* **141**:92–116.

Taavitsainen P, Kiukaanniemi K, and Pelkonen O (2000) In vitro inhibition screening of human hepatic P450 enzymes by five angiotensin-II receptor antagonists. *Eur J Clin Pharmacol* **56**:135–140.

Templeton IE, Thummel KE, Kharasch ED, Kunze KL, Hoffer C, Nelson WL, and Isoherranen N (2008) Contribution of itraconazole metabolites to inhibition of CYP3A4 in vivo. *Clin Pharmacol Ther* **83**:77–85.

Tornio A, Filppula AM, and Backman JT (2022) Translational aspects of cytochrome P450-mediated drug-drug interactions: A case study with clopidogrel. *Basic Clin Pharma Tox* **130**:48–59.

Tornio A, Filppula AM, Kailari O, Neuvonen M, Nyrönen TH, Tapaninen T, Neuvonen PJ, Niemi M, and Backman JT (2014) Glucuronidation Converts Clopidogrel to a Strong Time-Dependent Inhibitor of CYP2C8: A Phase II Metabolite as a Perpetrator of Drug-Drug Interactions. *Clin Pharmacol Ther* **96**:498–507.

Tornio A, Filppula AM, Niemi M, and Backman JT (2019) Clinical Studies on Drug-Drug Interactions Involving Metabolism and Transport: Methodology, Pitfalls, and Interpretation. *Clin Pharmacol Ther* **105**:1345–1361.

United States Food and Drug Administration. (2023) Drug Development and Drug Interactions: Table of Substrates, Inhibitors and Inducers.

United States Food and Drug Administration, Center for Drug Evaluation and Research (1998) Atacand clinical pharmacology and biopharmaceutics review. NDA 20-838:1-30.

United States Food and Drug Administration, Center for Drug Evaluation and Research. (2020) In vitro drug interaction studies — cytochrome P450 enzyme- and transporter-mediated drug interactions: guidance for industry.

VandenBrink BM and Isoherranen N (2010) The role of metabolites in predicting drug-drug interactions: focus on irreversible P450 inhibition. *Curr Opin Drug Discov Devel* **13**:66–77.

Walsky RL, Gaman EA, and Obach RS (2005) Examination of 209 drugs for inhibition of cytochrome P450 2C8. *J Clin Pharmacol* **45**:68–78.

Wang Y-H, Jones DR, and Hall SD (2004) Prediction of cytochrome P450 3A inhibition by verapamil enantiomers and their metabolites. *Drug Metab Dispos* **32**:259–266.

Yang J, Jamei M, Yeo KR, Rostami-Hodjegan A, and Tucker GT (2007a) Misuse of the well-stirred model of hepatic drug clearance. *Drug Metab Dispos* **35**:501–502.

Yang J, Jamei M, Yeo KR, Tucker GT, and Rostami-Hodjegan A (2007b) Prediction of Intestinal First-Pass Drug Metabolism. *Curr Drug Metab* **8**:676–684.

Yeung CK, Fujioka Y, Hachad H, Levy RH, and Isoherranen N (2011) Are Circulating Metabolites Important in Drug-Drug Interactions?: Quantitative Analysis of Risk Prediction and Inhibitory Potency. *Clin Pharmacol Ther* **89**:105–113.

Zamek-Gliszczynski MJ, Kalvass JC, Pollack GM, and Brouwer KLR (2009) Relationship between Drug/Metabolite Exposure and Impairment of Excretory Transport Function. *Drug Metab Dispos* **37**:386–390.

Address correspondence to: Dr. Aleksi Tornio, Institute of Biomedicine, University of Turku, and Unit of Clinical Pharmacology, Turku University Hospital, Kiinamyllynkatu 10, FI-20520 Turku, Finland. E-mail: aleksi.tornio@utu.fi

SUPPLEMENTAL DATA

Authors: Mikael O. W. Piha, Kristiina Cajanus, Marica T. Engström, Mikko Neuvonen, Troels K. Bergmann, Mikko Niemi, Janne T. Backman, Anne M. Filppula, Aleksi Tornio

Title: Candesartan Has No Clinically Meaningful Effect on the Plasma Concentrations of CYP2C8 Substrate Repaglinide in Humans

Drug Metabolism and Disposition: DMD-AR-2024-001798

Supplemental Methods

The liver-to-plasma ratios of candesartan and candesartan acyl-*β*-D-glucuronide in humans were predicted using Simcyp version 23 release 1 (Certara UK Limited, Sheffield, UK). The relevant input values, derived from either the literature or the present study, and the predicted liver-to-plasma ratios are presented in Supplemental Table 1.

The static interaction predictions (described in the main manuscript) were based either on the assumption that the liver-to-plasma ratios of candesartan and candesartan acyl-*β*-D-glucuronide were equal to 1, or on a worst-case scenario. Assuming a worst-case scenario, the predicted liver-to-plasma ratio (3.88; Supp. Table 1) was used for candesartan. For candesartan acyl-*β*-D-glucuronide, however, the predicted liver-to-plasma ratio was lower than 1 (Supp. Table 1). To avoid any underestimation of the drug-drug interaction risk, a ratio of 1 was used for candesartan acyl-*β*-D-glucuronide also in the worst-case static drug-drug interaction predictions.

SUPPLEMENTAL TABLE 1

Biochemical input parameters, and predicted liver-to-blood ratios of candesartan and candesartan acyl-*β*-D-glucuronide.

Parameter	Value	Reference/Comment
Candesartan		
molar mass (g/mol)	440.463	Chemicalize
log *P*	4.1	PubChem
pK_a	3.51 (acid)	Chemicalize
$f_{u,p}$	0.01	FDA, 1998
R_L[a]	3.8793	Predicted
Candesartan acyl-β-D-glucuronide		
molar mass (g/mol)	616	Chemicalize
log *P*	2.5	PubChem
pK_a	3.21 (acid)	Chemicalize
$f_{u,p}$	0.01	Present study
R_L[a]	0.53574	Predicted

a liver-to-plasma ratio

References

Chemicalize, https://chemicalize.com/ (Accessed: August 20, 2024)

National Center for Biotechnology Information (2024) PubChem Compound Summary for CID 2541, Candesartan. Retrieved August 20, 2024 from https://pubchem.ncbi.nlm.nih.gov/compound/Candesartan.

National Center for Biotechnology Information (2024) PubChem Compound Summary for CID 131769984, Candesartan O-glucuronide. Retrieved August 20, 2024 from https://pubchem.ncbi.nlm.nih.gov/compound/Candesartan-O-glucuronide.

United States Food and Drug Administration, Center for Drug Evaluation and Research (1998) Atacand clinical pharmacology and biopharmaceutics review. NDA 20-838:1-30. Retrieved April 25, 2023 from https://www.accessdata.fda.gov/drugsatfda_docs/nda/98/20838_ATACAND_biopharmr_P1.pdf.